International Journal of Biochemistry and Cell Biology 107 (2019) 154–165

Contents lists available at ScienceDirect

International Journal of Biochemistry and Cell Biology

journal homepage: www.elsevier.com/locate/biocel

Tachykinin NK1 receptor antagonist L-733,060 and substance P deletion exert neuroprotection through inhibiting oxidative stress and cell death after traumatic brain injury in mice

Qianqian Li[a], Xiao Wu[a], Yanyan Yang[a], Yue Zhang[a], Fang He[a], Xiang Xu[a], Ziwei Zhang[a], Luyang Tao[b], Chengliang Luo[b,*]

[a] School of Forensic Medicine, Wannan Medical College, Wuhu, 241002, Anhui, China
[b] Department of Forensic Medicine, Medical College of Soochow University, Suzhou, 215123, Jiangsu, China

ARTICLE INFO

Keywords:
Substance P
Traumatic brain injury
Neurokinin-1 receptor (NK1R)
Oxidative stress
Cell death

ABSTRACT

Substance P (SP) is believed to play a role in traumatic brain injury (TBI), and the inhibition of binding of SP to the tachykinin neurokinin-1 receptor (NK1R) using NK1R antagonists had made favorable effects on TBI. Our current study addresses the functional roles and underlying mechanisms of SP and NK1R antagonist L-733,060 following TBI. Adult male wild type C57BL/6 J and SP knock out (SP−KO) mice received a controlled cortical impact and outcome parameters were assessed. The results showed that TBI-induced motor and spatial memory deficits, lesion volume, brain water content and blood-brain barrier disruption were alleviated both in L-733,060-treated C57BL/6 J mice and vehicle-treated SP−KO mice. L-733,060 treatment and SP deletion inhibited TBI-induced the release of cytochrome c from mitochondria to cytoplasm, activation of caspase-3, oxidative stress and neuroinflammation. Higher SP levels in serum and cortex were observed in wild type mice undergoing TBI relative to wild type sham group, but very little expression of cortical SP was detected in the SP-/- mice either TBI or not. Upregulation of NK1R expression after TBI was observed, and there was no significant difference between wild type and SP−KO groups. *in vitro*, L-733,060 and SP deletion inhibited scratch injury-induced cell death, loss of mitochondrial membrane potential and reactive oxygen species (ROS) production following TBI. Together, the results of this study implicate a functional role for NK1-R antagonist L-733,060 and deletion of SP in TBI-induced neurological outcome, oxidative damage, neuroinflammation and cell death. Upregulation of NK1R maybe a consequence of TBI, independent of the levels of substance P. This study raises the possibility that targeting SP through its receptor NK1R or genetic deletion may have therapeutic efficacy in TBI.

1. Introduction

Traumatic brain injury (TBI), the leading cause of morbidity and mortality in people under 40 years old, remains a significant medical concern worldwide as a considerable cause of death and permanent disability, imposing a significant burden on society (Jin et al., 2015). Despite the enormity of this public health problem, no effective therapies for TBI currently exist. The hope for an effective treatment is derived from the fact that much of the post-traumatic damage to the injured brain is caused by a secondary injury cascade of consecutive pathological and pathophysiological events including blood–brain barrier (BBB) opening, edema formation, excitotoxicity, activation of inflammatory responses, oxidative stress and ultimately cell death that exacerbates the primary mechanical TBI (Mustafa et al., 2010). In particularly, inflammation is thought to contribute to much of the secondary cell injury following TBI, directly injuring cells, and facilitating other injury factors such as oxidative stress (Liao et al., 2013) and edema Formation (Chodobski et al., 2011).

Substance P (SP) is a member of the tachykinin family of neuropeptides, which are widely distributed throughout the central nervous system (CNS) and actively involved in inflammatory processes. SP is released early following acute injury to the CNS such as TBI, promoting

Abbreviations: BBB, bloodbrain barrier; CCK-8, Cell Counting Kit-8; CNS, central nervous system; C57, C57BL/6; cyt-c, cytochrome c; EB, Evans blue; ELISA, Enzyme-Linked Immune-Sorbent Assay; LDH, lactate dehydrogenase; MDA, Malondialdehyde; MWM, Morris Water Maze; NAT, N-acetyl-L-tryptophan; NK1R, neurokinin-1 receptor; PCNs, primary cortical neurons; ROS, reactive oxygen species; SP, Substance P; TBI, traumatic brain injury

* Corresponding author at: Department of Forensic Medicine, Medical College of Soochow University, 178 Ganjiang East Street, Suzhou, 215123, China.
E-mail address: clluo@suda.edu.cn (C. Luo).

https://doi.org/10.1016/j.biocel.2018.12.018
Received 10 September 2018; Received in revised form 22 December 2018; Accepted 25 December 2018
Available online 26 December 2018
1357-2725/ © 2018 Elsevier Ltd. All rights reserved.

a neurogenic inflammatory response characterized by an increase in the permeability of the BBB and the development of vasogenic edema (Donkin et al., 2009). Serum SP levels were associated with injury severity and mortality in patients with severe TBI, indicating that serum SP levels could be used as a biomarker to predict mortality in patients with severe TBI, and may be of great pathophysiological significance in patients with TBI (Lorente et al., 2015). SP expression was increased at 30 min following rodent TBI in perivascular tissue (Donkin et al., 2009) with such increases still evident at 24 h and 3 days post-TBI (Cook et al., 2009; Donkin et al., 2009).

SP is known to preferentially bind to the tachykinin neurokinin-1 receptor (NK1R), activation of which leads to increased BBB permeability and edema development (Vink et al., 2003). Whereas, the inhibition of binding of SP to the NK1R using NK1R antagonist N-acetyl-L-tryptophan (NAT), had made favorable effects on Parkinson's disease (Thornton and Vink, 2012), cerebral ischemia (Yu et al., 1997), spinal cord injury (Leonard and Vink, 2013) and TBI (Vink and van den Heuvel, 2010). Specifically, NAT promotes a beneficial response post-injury, presumably by competitive antagonism with SP for the NK1 receptor. This action via the NK1 receptor was confirmed with the inactive D-enantiomer of NAT, which had no significant effect on motor outcomes after TBI, ruling out the possibility of non-specific effects playing a major role (Donkin et al., 2011). In addition, substance P primes polymorphonuclear cells for oxidative metabolism (superoxide production) (Hafstrom et al, 1998), thus providing a source of reactive oxygen species (ROS) known to exacerbate the injury process. Oxidative stress plays a vital role in secondary injury caused by TBI, not only because of the excessive production of ROS but also due to the exhaustion of antioxidant defense enzymes, such as SOD, GPx and catalase (Özay et al., 2017).

Although these findings in TBI models are extremely encouraging, very few reports using SP knock out mouse describing the direct role of substance P in TBI models had been published. By comparing C57BL/6 J wild type mice and the SP−KO (SP-/-) mice, this study was designed to provide the direct evidence for the effects of substance P on TBI-induced neurological behavior outcome, lesion volume, edema development, BBB disruption, oxidative stress, inflammatory response and cell death, etc. To investigate the underlying mechanism whether the SP/NK1R system involves various biological functions, the effects of NK1R antagonist L-733,060 on various parameters following TBI and the changes of SP/NK1R expression were assessed. In addition, the effects of L-733,060 and deletion of SP on *in vitro* TBI-induced cell death and ROS production were also detected.

2. Materials and methods

2.1. Animals and drug administration

Adult male C57BL/6 J mice with an average body weight of 23 g (20–25 g) were purchased from the Animal Center of the Chinese Academy of Sciences, Shanghai, China. SP−KO male mice (SP-/-: B6.Cg-*Tac1*^{tm1Bbm}/J, Stock No: 004103), weighing 20 to 25 g, were purchased from the Jackson Laboratory. L-733,060 (Cat. No. 1145), a BBB-permeable selective NK1 antagonist, was purchased from Tocris Bioscience. L-733,060 (10 mg/kg, i.p.) was given 30 min after TBI, and daily for up to 16 days. The dose of L-733,060 was determined based on previous study (Dang et al., 2018). Healthy male C57BL/6 J and SP−KO (SP-/-) mice were coded and assigned randomly to 6 groups: C57BL/6 J vehicle sham group, C57BL/6 J L733,060 sham group, SP-/- vehicle sham group, C57BL/6 J vehicle TBI group, C57BL/6 J L-733,060 TBI group and SP-/- vehicle TBI group. The mice in C57BL/6 J vehicle TBI group and SP-/- vehicle TBI group were intraperitoneally injected with an equivalent volume of sterile saline 30 min after TBI.

2.2. Mouse TBI model

Animal experiments or procedures were approved by the Ethics Committee of Soochow University and Wannan Medical College, and were in compliance with the National Institutes of Health (NIH) guidelines for Laboratory Animal Use and Care. All attempts were made to minimize animal suffering and the number of animals used. The procedure of mouse TBI model was described and used in detail previously (Luo et al., 2010, 2011; Wu et al., 2016). Briefly, adult male mice were deeply anesthetized with chloral hydrate (4% solution) and mounted in a Kopf stereotaxic system (David Kopf Instruments, Tujunga, California). All steps were all performed under aseptic conditions and using aseptic techniques. A midline skin incision on the scalp was performed to expose the skull, and a 5-mm diameter manual trephine (Roboz Surgical Instrument Co., Gaithersburg, MD) was carefully used to penetrate the skull for removal of the bone flap. Mice were subjected to TBI in left part of the brain (bone flap centered at the bregma + 3.0 mm, lateral left 2.7 mm) using a weight-drop device, a 40 g weight dropped from 20 cm onto a 2 mm diameter footplate resting on the dura with a controlled depth of 1.0 mm, as described previously (Luo et al., 2010, 2011). The reproducibility and consistency of this TBI model were ensured and the craniotomy was closed immediately after TBI (Luo et al., 2011). At 30 min, 5 h and 24 h after TBI, the mice were anesthetized with chloral hydrate and blood samples were obtained from direct puncture of the heart with a heparinized syringe. The brain was then removed and stored at −80 °C for further analyses. For the sham operation group, only the surgical procedure was performed on animals without cortical impact. The procedures were conducted by the same person in order to minimize the variance in operation, and data were obtained by investigators blinded to study group.

2.3. Motor function and Morris water maze testing

Motor function testing was first evaluated using a wire-grip test (also called pole climbing test) from day 1 to day 7 after TBI, according to the procedure described previously (Bermpohl et al., 2006; Luo et al., 2010). Briefly, mice were placed on a metal wire (100 cm long) suspended 45 cm above a foam pad, and were allowed to traverse the wire for 60 s. The latency that a mouse remained on the wire within a 60 s' interval was measured and recorded. Wire-grip scores were quantitated using a five-point scale and the manner in which it held on (one to four paws, tail, paws plus tail) was scored (Bermpohl et al., 2006). The wire-grip test was conducted in triplicate and the average score of three trials per day was calculated for each mouse.

Motor strength and coordination were then determined using a rotarod test (Acceler Rota-Rod 7650, Italy) as previously described (Park et al., 2014). The rotarod test using accelerating paradigms is widely preferred in TBI research. Prior to surgery, the C57/BL6 and SP-/- mice were trained for balancing on the rotating drum for three days. Accelerating rotarod was performed by placing mice on rotating drums and measuring the time that each animal could maintain its balance on the rod. The rotarod was accelerated from 4 to 40 r.p.m. for 300 ss as preoperative baseline (5-min period). The test was carried out on days 1–7 and day 14 after TBI surgery. Animal was given three trials per day and the average latency without falling off the accelerating drum was recorded (Park et al., 2014). The "latency to fall" is typically used as a quantitative endpoint to evaluate motor function.

Morris water maze (MWM) task was conducted to evaluate spatial learning and memory performance after insults as described previously (Bermpohl et al., 2006; Mannix et al., 2011). In brief, the water in the tank (120 cm in diameter, 50 cm high) was colored by white non-toxic food pigment and a clear plexiglass goal platform 5 cm in diameter was positioned 0.5 cm below the water's surface approximately 15 cm from the southwest wall. For the place navigation test, mice were allowed a maximum of 90 s to find the submersed platform on days 8–15. Once the mouse reached the submersed platform, it would be allowed to

remain on the platform for an additional 10 s. If the mouse failed to find the submersed platform within 90 s, the investigator would guide to the platform and the mouse was allowed to stay on the platform for 30 s. The escape latency (the time to reach the visible platform) was automatically recorded and analyzed by a video/compute system. For the spatial probe test, the submersed platform was removed from the pool on day 16. Each mouse was allowed to explore the pool within 90 s and the frequency of passing through the target quadrant was monitored by a video tracking system and analyzed with a tracking device and software (Chromotrack 3.0, San Diego Instruments).

2.4. Lesion volume measurements

The animals which had received TBI were sacrificed on days 1, 7 and 17 following TBI. The brains were quickly removed, fixed for 12 h, and then cryoprotected in 15% sucrose. The brains were coronally sectioned into 12-μm-thick slices, and then stained with Cresyl Violet. Lesion volume was quantitatively analyzed with Sigma Scan Pro 5 and the average value in microliters for each group was calculated (Wu et al., 2016). Lesion volume was then expressed in cubic millimeters in the injured hemisphere and as percentage volume of the non-injured hemisphere.

2.5. Brain water content measurements

Brain water content was measured with a wet-dry weight method at 24 h after TBI, as previously reported (Cui and Zhu, 2015). Briefly, the mice were anesthetized with 4% chloral hydrate and decapitated at 24 h post TBI. The whole brain was removed and divided into the right and left hemispheres that separated along the anatomic midline. The wet weight of each hemisphere was measured on an electronic analytical balance. The tissues were completely dried in an oven at 100 °C for 24 h, and the dry weight of each hemisphere was then determined. The brain edema/the percentage water content (% water) was calculated according to the following Elliott formula for each hemisphere: (wet weight-dry weight)/wet weight × 100.

2.6. Measurement of Evans blue extravasation

The BBB permeability was evaluated by measuring the extravasation of Evans blue (EB) dye at 24 h following TBI, as described previously (Belayev et al., 1996; Yuan et al., 2016). The Evans blue dye (2%; 2 mL/kg body weight) was intravenously administered via the tail vein 30 min before the mice were sacrificed. Then, the mice (n = 6/group) were perfused with phosphate-buffered saline (PBS) through the left ventricle, and brain specimens were collected and rapidly weighed. After removal of intravascular-localized dye, the brain was divided into the ipsilateral and contralateral hemispheres. Each sample was weighed immediately and incubated in formamide (1 ml/100 mg). Following incubating at 60 °C for 24 h, the homogenate was centrifuged at 5 000 rpm for 10 min. The supernatant was collected, and the absorbance was measured with a spectrophotometer at 620 nm. The EB leakage was expressed as micrograms per gram of brain tissue.

2.7. Protein extraction

Each injured cortical ($2 \times 2 \times 2\,mm^3$ tissue block including the impact site and surroundings) from each mouse was dissected for several assays (Wu et al., 2018). The samples were lysed in RIPA lysis and extraction buffer containing PMSF and protease inhibitor (Thermo Fisher Scientific, USA). The lysates were centrifuged for two times at 12,000 g for 20 min at 4 °C, and the supernatants were collected. The concentration of protein in each lysate was detected using a BCA Quick Start™ Bradford protein assay kit (Bio-Rad Laboratories, Inc.).

Isolation of mitochondria was performed using a mitochondria/cytosol fractionation kit (Biovision, USA) according to the manufacturer's instructions. In Brief, each cortical sample was washed with ice-cold PBS, and resuspended in cytosol extraction buffer mix, and then dounce-homogenized. To pellet nuclei, the homogenate was centrifuged at 1000 g at 4 °C for 10 min and the resultant supernatant was transferred to a new clear Eppendorf tube. The supernatant was centrifuged at 12,000 g at 4 °C for 30 min to obtain the mitochondrial pellet and supernatant. The resulting supernatant was collected as the cytosolic fraction. The pellet was lysed in Mitochondrial Extraction Buffer Mix and collected as the mitochondrial fraction.

2.8. Western blot analysis

Western blot analysis was performed to assess protein levels as described previously (Luo et al., 2011). In brief, proteins (20 μg) from the lysates were resolved by SDS-PAGE gen using a constant current and then transferred to PVDF membranes on a semidry electrotransferring unit (Bio-Rad). Membranes were incubated with primary antibodies to anti-NK1R antibody (1:500-1000, NB300-119, Novus Biologicals), Cytochrome C (Abcam, ab110325, 1:500), COX IV (Abcam, ab16056, 1:1000), anti-caspase-3 (1:500, bioworld), anti-substance P (1:500, Invitrogen), β-actin (CMCTAG, AT0001, 1:2000) and Hsp60 (Abcam, ab46798, 1:1000) overnight at 4 °C. The membranes were then washed and incubated with horseradish peroxidase-conjugated secondary antibodies (1:2,000) for 2 h. Immunoreactivity was detected using the ECL chemiluminescence system (ChemiScope, Shanghai). Protein bands were scanned and density was analyzed using the ChemiScope analysis.

2.9. Malondialdehyde (MDA) content and the activities of SOD and GPx

The MDA content and the activities of SOD and GPx were assessed with a spectrophotometer, using the appropriate kits (BioAssay Systems, CA, USA), according to the manufacturer's instructions. Total protein concentration was determined by the Bradford method. The MDA level and the activities of SOD and GPx were expressed as nmol/mg protein and U/mg protein, respectively (Liang et al., 2018).

2.10. Cytokine enzyme-linked immune-sorbent assay (ELISA)

The levels of inflammatory cytokines in serum were detected by TNF-α and IL-1β ELISA kits (Biolegend, USA), according to the manufacturer's protocols. Absorbance was read at 450 nm. Determinations were performed in triple, and the results were expressed as mean OD ± SEM.

2.11. The parameter substance P immunoassay

At 30 min, 5 h and 24 h post-TBI, injury blood was collected from the tail vein. The serum was isolated by centrifugation at 3000 rpm for 10 min. Substance P levels in the serum was measured using Substance P Parameter Assay Kit (KGE007, R&D Systems) according to the manufacturer's instructions. Briefly, serum was collected in tubes and diluted in a ratio of 1:2 in an assay buffer. After samples were plated into individual wells on a 96-well plate, 50 μL of primary antibody solution and 50 μL of conjugate were then added to each well. The plates were then incubated for 3 h at room temperature on a horizontal orbital microplate shaker. The sample wells were then aspirated and washed thrice. A volume of 200 μL substrate solution was then added and incubated for 30 min at room temperature. Finally, stop solution was added to each well, and the optical density of each well to be determined using a microplate reader set at 450 nm with the wavelength correction set between 540 and 570 nm (Donkin et al., 2009).

2.12. Primary cortical neuron culture and in vitro TBI model

Primary cortical neuron (PCN) were isolated from E14 to E16 C57BL/6 and SP−KO (SP-/-) mouse embryos. The cortices were

harvested in dissociation medium containing trypsin (0.25%, Invitrogen) to digest tissues, and then triturated. Neurons were maintained in Neurobasal medium (Invitrogen) supplemented with B27 (2%, Invitrogen), glutamine (1%, Invitrogen), glutamate (25 μM, Sigma), penicillin (100 U/ml)/streptomycin (50 μg/ml, Invitrogen). Neurons were then seeded into 96-well plates (Falcon) and 24-well plates (Falcon), which were precoated with poly-L-lysine (Sigma, USA), and put into a 37 °C humidified incubator (Taibai Espec) with a 5% CO_2 in air. The purity of neurons was identified by immunostaining for MAP2 (a neuronal-specific marker) and indicated that 90–95% of cells in cultures were MAP2 positive. There maining cells exhibiting morphological characteristics of glial cells were verified by GFAP immunostaining. The method was used as described previously (Luo et al., 2013, 2015).

To imitate *in vivo* TBI model, the scratch cell injury was induced on day 7 as an *in vitro* TBI model in cultured primary cortical neurons (Han et al., 2014; Mori et al., 2002). Briefly, 96-well plates were manually scratched with a plastic stylet needle (10 μl) following a 2 × 2 square grim, and 24-well Petri dishes were scratched with a 10 μl plastic stylet needle following a 4 × 4 square grim. For the sham group, no scratch injury was performed.

2.13. Lactate dehydrogenase assay

Cell death or cytotoxicity was quantitatively evaluated using the lactate dehydrogenase (LDH) assay according to the manufacturer's instructions. PCNs were pretreated with L-733,060 (from 0.001 nM to 100 μM) dissolved in 0.1% DMSO 2 h before scratch cell injury. The release of LDH into the culture media was detected at 20 h after scratch cell injury using a LDH-Cytotoxicity Assay Kit II (ab65393, Abcam, USA). Briefly, sample preparation and sample incubation were performed following the manufacturer's instructions. The cells were centrifuged at 600 g at 4 °C for 10 min and the resultant supernatant was transferred to a clear 96-well plate. LDH Reaction Mix was added to each well, and then mixed and incubated for 30 min at room temperature. Absorbance was measured at 450 nm using a microtiter plate spectrophotometer (Bio-Rad Laboratories, CA, USA). LDH leakage was calculated as follows: LDH leakage (%) = (Test Sample - Low Control) / (High Control – Low Control) × 100.

2.14. Assessment of neuronal viability

Cell viability was determined using the CCK-8 Kit (Sigma-Aldrich, USA) following the manufacturer's instructions. Neurons were treated with L-733,060 dissolved in 0.1% dimethyl sulfoxide (DMSO) at 2 h before scratch cell injury. At 20 h following injury, the cells in every well were treated with 10 μL CCK-8 solution, and incubated for another 3 h at 37 °C in a humidified incubator in 5% CO_2. The absorbance values were measured at 450 nm using a microplate reader (Ji et al., 2012).

2.15. Intracellular ROS assay

The levels of intracellular ROS generation were determined by DCFH-DA as described previously (Wu et al., 2018). Briefly, following washing with 1 × PBS, neurons were loaded with DCFH-DA (10 μM in colorless DMEM) at 30 °C for 30 min. Fluorescence was assessed by using a fluorescence spectrophotometer with excitation at 485 nm and emission at 530 nm.

2.16. Determination of mitochondrial transmembrane potential (ΔΨm)

Living neurons were stained with rhodamine 123 (Rh 123, Molecular Probes) and tetramethylrhodamine methyl ester (TMRM, Molecular Probes) at room temperature for 10 min, as previously described (Luo et al., 2015). Both Rh 123 and TMRM were purchased from Molecular Probes, and digital images were taken.

2.17. Measurement of cellular ATP

The levels of cellular ATP contents were assessed by using a firefly luciferase ATP assay kit (Calbiochem, Germany), according to the manufacturer's instructions. Different concentrations of ATP (0.1 ng–100.0 ng) were used and standard curve was prepared. Optical density was determined on a plate reader at 562-nm wavelength.

2.18. Statistical analysis

All the experiments were randomized and performed in a blinded manner. The data were expressed as mean ± SEM in each group, and were analyzed using GraphPad Prism 5 Software (La Jolla, CA, USA). All data are based on at least three independent experiments. Statistical analysis was given using two-way analysis of variance (ANOVA), followed by Tukey's post hoc test to determine significance values between different experimental groups. For all comparisons, statistical significance was defined as $P < 0.05$.

3. Results

3.1. L-733,060 and deletion of substance P alleviated TBI-induced motor and spatial memory tasks deficits

Using a wire-grip test, TBI elicited a significant decline in motor performance at 1–7 days post-injury. NK1R antagonist L-733,060 exerted the improvement on days 1–7 after TBI, compared with vehicle C57BL/6 J mice. Additionally, the recovery of motor functional outcome during the period in vehicle SP-/- mice was better than that in vehicle C57BL/6 J mice (Fig. 1A).

Rotarod performance was utilized as the motor strength and coordination outcome measure. Prior to the induction of injury, the mean rotarod score of all animals was 300 s. Following injury, there was a significant decline in vehicle-treated C57BL/6 J mice, to 62 ± 13 s at 1 day post-injury (Fig. 1B). These vehicle-treated C57BL/6 J mice showed improvement over the 14-day assessment period, but there was a significant difference on days 1–7 between vehicle-treated C57BL/6 J group and the sham group. NK1R antagonist L-733,060 exerted the improvement in rotarod performance on days 1–7, relative to the vehicle C57BL/6 J mice (Fig. 1B). Moreover, a profound improvement in rotarod score was observed in the vehicle SP-/- mice, comparing to vehicle C57BL/6 J mice on days 1–6 (Fig. 1B; $P < 0.05$).

Morris-water maze tasks were then utilized to test spatial memory ability on days 8–15. As shown in Fig. 1C, vehicle-treated C57BL/6 J mice displayed increased latencies in the ability to find the hidden platform, versus the sham group on days 8–15. NK1R antagonist L-733,060 inhibited the upregulation of latencies on days 10–15, compared with vehicle-treated C57BL/6 J mice (Fig. 1C; $P < 0.05$). A significant decrease in the latencies was also observed in the vehicle SP-/- group, relative to vehicle C57BL/6 J mice on days 10–14 (Fig. 1C; $P < 0.05$). As far as spatial probe test was concerned, on day 16 post TBI, the frequency of passing through the platform quadrant was significantly lower in vehicle C57BL/6 J group than that in the sham group. L-733,060 treatment inhibited the downregulation of the frequency, compared with vehicle C57BL/6 J mice. A significant decrease in the probe tests was also reversed in SP-/- mice, relative to vehicle C57BL/6 J mice (Fig. 1D).

3.2. L-733,060 and deletion of substance P mitigated TBI-induced lesion volume, brain edema and BBB leakage

The study was then designed to assess the cumulative loss of brain tissue on days 1, 7 and 17. The results showed that TBI caused profound tissue loss in the brain on day 7 and 17, relative to the sham group. L-

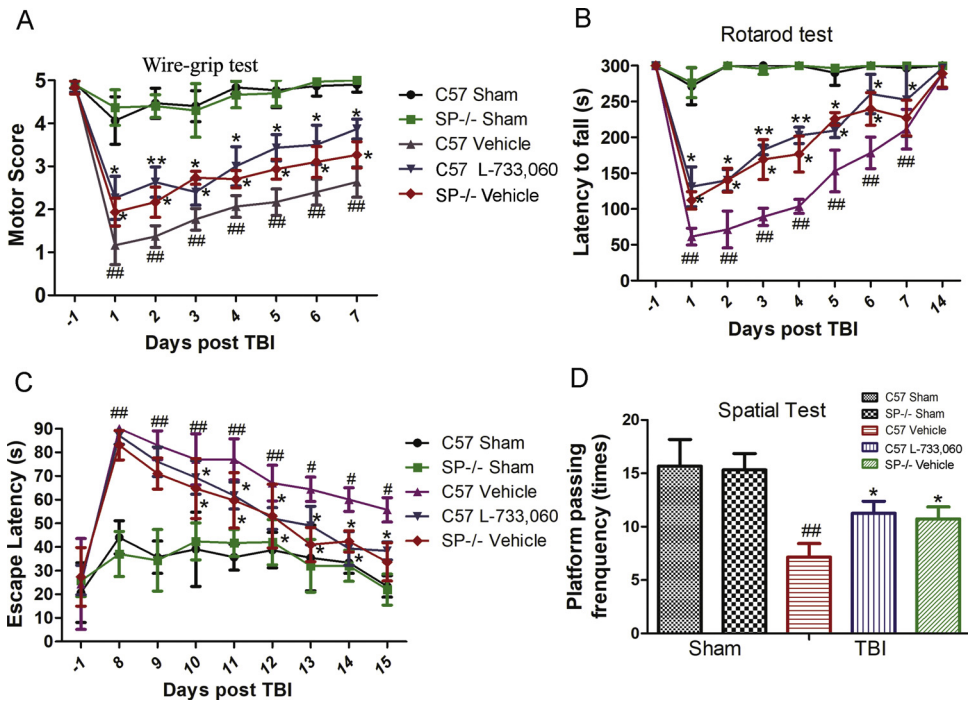

Fig. 1. L-733,060 and knock out of substance P alleviated TBI-induced behavioral deficits including motor and spatial memory tasks deficits. (A) Motor function test was performed 1–7 d after injury (n = 8). Motor impairment was first observed as revealed by decreases in motor performance using Wire-grip test and no differences were observed among five groups in baseline motor function. While compared with C57BL/6 J vehicle group, the recovery of motor function deficits speeded up in the SP-/- vehicle mice. (B) Rotarod performance (Latency to fall) was also used as the motor strength and coordination outcome measure on days 1–7 and 14 (n = 8). (C) Latency to find the hidden platform was measured on days 8–15 (n = 8). (D) As far as spatial probe test was concerned, on day 16 post TBI, the frequency of passing through the platform quadrant was observed (n = 8). *P < 0.05 or **P < 0.01 vs. vehicle C57BL/6 J group; #P < 0.05 or ##P < 0.01 vs. sham group. C57, C57BL/6 J. SP-/-. SP−KO.

733,060 treatment reduced the lesion volume on day 17, relative to vehicle C57BL/6 J mice. On day 17, a significant decrease in the lesion volume was also observed in the vehicle SP-/- group, compared with the vehicle C57BL/6 J mice (Fig. 2A; $P < 0.01$).

Following TBI, the water content of the injured hemisphere increased in vehicle-treated C57BL/6 J group at 24 h post injury, compared with the sham group (Fig. 2B). Intraperitoneal injection of L-733,060 ameliorated brain edema in C57BL/6 J mice. Compared with vehicle C57BL/6 J mice, TBI-induced brain edema was ameliorated in the vehicle SP-/- group (Fig. 2B). Meanwhile, L-733,060 alone did not alter the water content in C57BL/6 J sham mice as compared to vehicle sham control (Fig. 2B).

To evaluate BBB permeability after TBI, Evans blue (EB) extravasation was conducted at 24 h following TBI. As shown in Fig. 2C, compared to the sham group, EB concentration increased significantly in vehicle treated C57BL/6 J mice. In contrast, L-733,060 treatment decreased EB leakage in vehicle treated C57BL/6 J mice (Fig. 2C). TBI-induced EB leakage was also mitigated in the vehicle SP-/- mice, relative to vehicle C57BL/6 J mice. Meanwhile, L-733,060 alone did not alter EB leakage in C57BL/6 J sham mice as compared to vehicle sham control (Fig. 2C).

3.3. L-733,060 and deletion of substance P inhibited TBI-induced mitochondria mediated apoptotic pathway

We next assessed blotting for cytochrome c (cyt-c) in purified mitochondria. A significant reduction in protein levels of cyt-c in mitochondrial fraction and a concomitant increase in cyt-c levels in cytosolic fraction were observed in vehicle-treated C57BL/6 J group, relative to the sham group (Fig. 3A-C). L-733,060 treatment inhibited the release of cyt-c in the vehicle-treated C57BL/6 J group. Moreover, deletion of substance P significantly inhibited TBI-induced release of cyt-c from mitochondria to cytosol, compared to the C57BL/6 J vehicle mice (Fig. 3A-C).

The release of cytochrome c from mitochondria triggers activation of downstream caspases. Western blot analysis demonstrated that the upregulation of cleaved caspase-3 after 24 h post-TBI was observed both in vehicle-treated C57BL/6 J and SP-/- groups, relative to their respective sham group (Fig. 3D and E). Whereas, L-733,060 treatment inhibited the upregulation of cleaved-caspase-3 in the vehicle-treated C57BL/6 J group. A significant decrease in the levels of cleaved caspase-3 was observed in SP-/- vehicle group, comparing to C57BL/6 J vehicle group (Fig. 3A-C).

3.4. L-733,060 and deletion of substance P inhibited TBI-induced oxidative stress and neuroinflammation

To evaluate the effect of SP on oxidative stress following TBI, indicators of lipid peroxidation and antioxidant levels (e.g., MDA level, activities of SOD and GPx) were assessed. Following TBI, the MDA level was increased both in the C57BL/6 J vehicle group and the SP-/- vehicle group, compared with their respective sham group. This effect was mitigated by L-733,060 treatment in C57BL/6 J group or deletion of SP in SP−KO group (Fig. 4A). Comparing to the sham group, the activities of GPx (Fig. 4B) and SOD (Fig. 4C) were both decreased in C57BL/6 J vehicle TBI group, while their activity increased in L-733,060-treated C57BL/6 J group and in vehicle-treated SP-/- group (Fig. 4B and C). In addition, a significant decrease of SOD activities after TBI was observed in vehicle-treated SP-/- group, relative to the sham SP-/- group (Fig. 4B).

To investigate the effect of SP on the inflammatory response after TBI, ELISA was carried out to assess the levels of inflammatory cytokines. The results showed that a significant increase of serum IL-1β and TNF-α expression at 24 h post-TBI was observed, relative to the respective sham group. While both L-733,060 treatment and deletion of SP significantly inhibited the upregulation of IL-1β (Fig. 4D) and TNF-α (Fig. 4E) levels.

3.5. The changes of serum SP concentration, and the levels of SP and NK1R expression in cortex after TBI

Given SP may be involved in TBI-induced biological changes the mentioned above, it was of interest to establish whether SP was detected in the blood after TBI. Accordingly, we used a competitive ELISA assay to determine SP concentration within serum samples of injured animals at 30 min, 5 h and 24 h after injury (Fig. 5A). In the C57BL/6 J mice, SP concentration increased at 30 min post-TBI and peaked at 5 h, then declined but remained elevated at 24 after TBI.

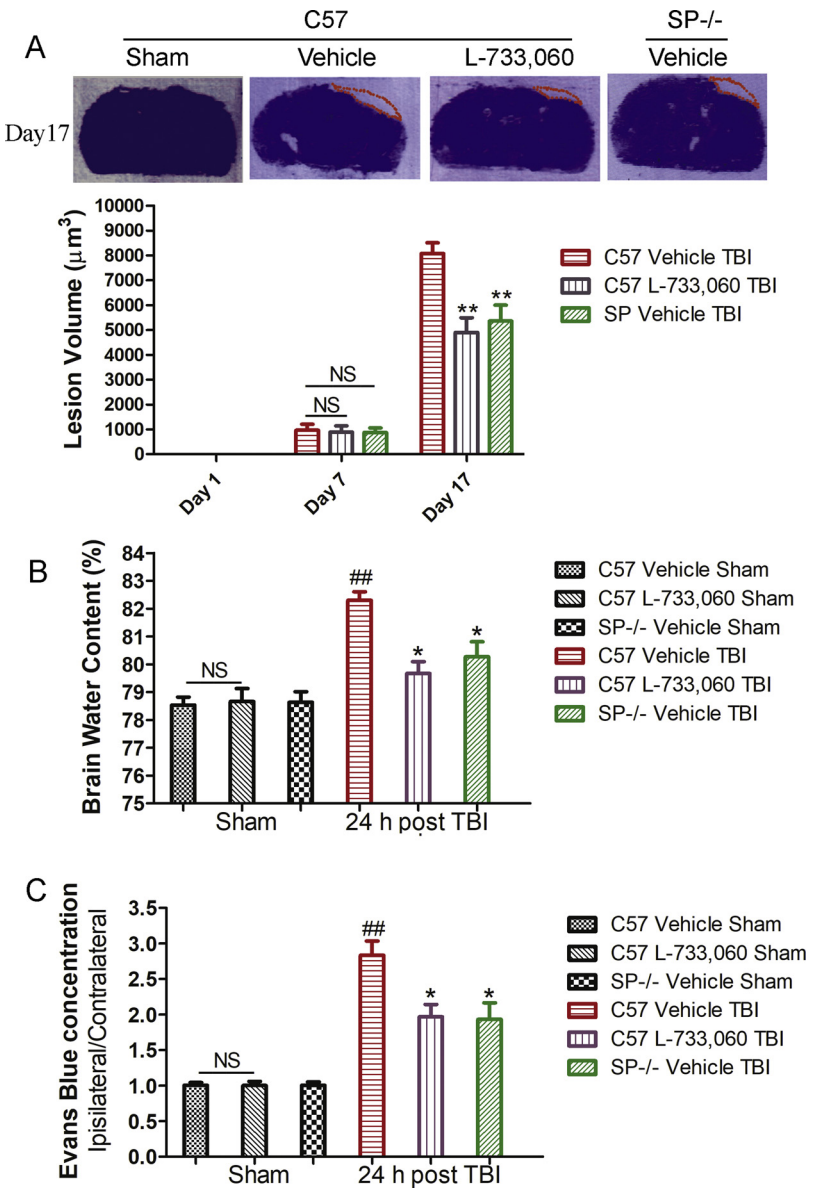

Fig. 2. L-733,060 and deletion of substance P mitigated TBI-induced lesion volume, brain edema and BBB leakage. (A) All animals were sacrificed on days 1, 7 and 17 after TBI (n = 8). 500-μm Brain sections from the entire brain stained with Cresyl Violet. The areas of the lesion, both injured and non-injured hemisphere, were determined using an image analysis system. Lesion volume was quantitatively analyzed with Sigma Scan Pro5. $^{**}P < 0.01$ vs. C57BL/6 J vehicle TBI group. (B) The water content of injured hemisphere and heterolateral hemisphere were measured at 24 h after TBI (n = 6). $^{\#\#}P < 0.01$ vs. C57BL/6 J vehicle sham group. $^{*}P < 0.05$ vs. C57BL/6 J vehicle TBI group. (C) The bar graph shows a quantitative analysis of the Evans blue staining at 24 h post TBI (n = 6). $^{\#\#}P < 0.01$ vs. C57BL/6 J vehicle group. $^{*}P < 0.05$ vs. C57BL/6 J vehicle TBI group. C57, C57BL/6 J. NS, No significance.

The blots for substance P and its receptor NK1R were then performed. Very little expression of SP was detected in the sham SP-/- mice, compared with the sham wild type mice (Fig. 5B and C). Following TBI, a significant increase was observed in the vehicle wild type mice, relative to the sham wild type mice, but there was no significant difference between the vehicle SP-/- mice and the sham SP-/- mice. Moreover, there was a significant difference in the expression of SP at 24 h post-TBI between the wild type and SP-/- groups (Fig. 5B and C). As shown in Fig. 5B and D, the upregulation of NK1R expression was observed both in the vehicle-treated C57BL/6 J mice and the vehicle-treated SP-/- mice, compared with respective sham groups ($P < 0.01$). Whereas, there was no significant difference in the expression of NK1R at 24 h after TBI between the wild type and SP-/- groups (Fig. 5B and D, $P > 0.05$).

3.6. L-733,060 and knockout of substance P inhibited in vitro TBI-induced cell death and reactive oxygen species (ROS) production

To determine whether L-733,060 exerts a protective effect on *in vitro* neuronal injury in wild type group, and to find the optimum concentration range of L-733,060, we first investigate the effects of L-733,060 on cell viability by LDH assay. Using LDH assay, exposing PCNs to scratch cell injury with L-733,060 (1 nM to 100 μM) resulted in significant dose-dependent inhibition of cell death (Fig. 6A). Plotting the dependence between drug concentration and scratch injury-mediated PCN cell death as a semi-log plot revealed the EC50 to be 13.2 nM, with maximum protection 53% (Fig. 6B).

To further determine the effects of L-733,060 and SP deletion on PCNs undergoing scratch injury, two types of PCNs were used which obtained from embryonic 14 to 16-day-old C57BL/6 J mice and SP-/- mice, respectively. Using CCK-8 assay, L-733,060 (10 μM) treatment significantly attenuated cell death in C57BL/6 J group after insults (Fig. 6C). Exposing PCNs in the SP-/- group to scratch cell injury showed significant inhibition of cell death, relative with PCNs in C57BL/6 J group. Meanwhile, L-733,060 (10 μM) alone did not alter cell survival in C57BL/6 J sham group as compared to vehicle sham control (Fig. 6C).

We further investigated the role of L-733,060 and SP deletion in ROS production after scratch cell injury. As shown in Fig. 6D, compared to the sham cells ($P < 0.01$), the fluorescence intensity increased significantly in cells of the C57BL/6 J vehicle group after injury, indicating that scratch cell injury gave rise to mitochondrial ROS production.

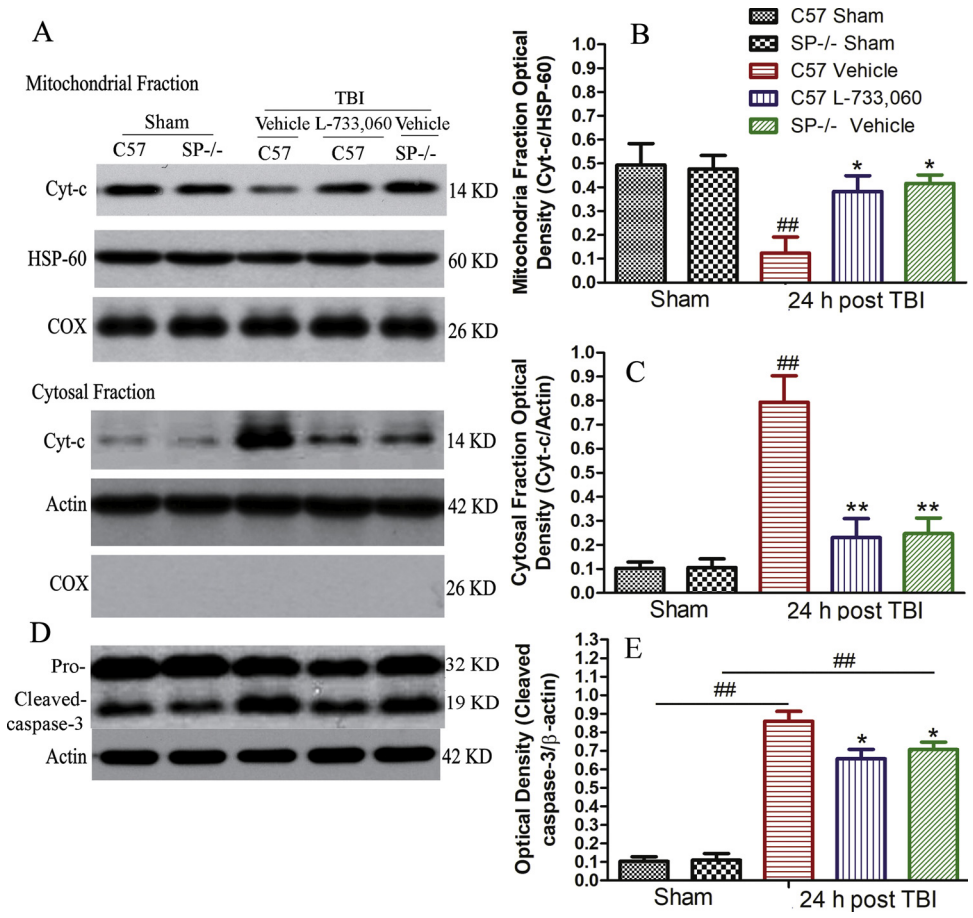

Fig. 3. L-733,060 and deletion of substance P inhibited TBI-induced mitochondria mediated apoptotic pathway. (A) Each cortical sample at 24 h after TBI was homogenized and centrifuged for isolation of mitochondrial and cytosolic fractions. (B, C) Optical densities of the protein bands were analyzed with ChemiScope analysis and normalized with loading control (HSP-60, β-actin). Bars represent mean ± SEM (n = 4). $^{\#\#}P < 0.01$ vs. sham group and $^{*}P < 0.05$ or $^{**}P < 0.01$ vs. C57BL/6 J vehicle TBI group. (D) Cleaved caspase-3 protein levels were detected with immunoblotting at 24 h post TBI. (E) Optical densities of the protein bands were analyzed with ChemiScope analysis and normalized with loading control (β-actin). Bars represent mean ± SEM (n = 4). $^{\#\#}P < 0.01$ vs. respective sham group and $^{*}P < 0.05$ vs. C57BL/6 J vehicle TBI group. C57, C57BL/6 J. SP-/-. SP−KO.

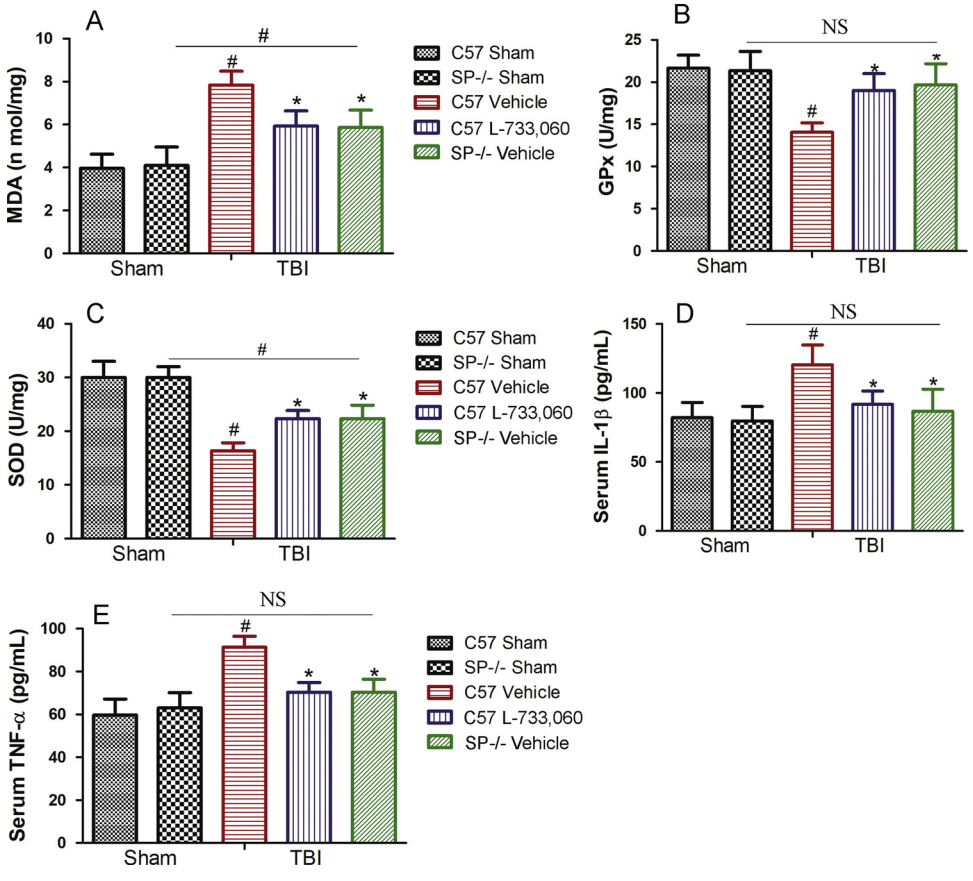

Fig. 4. L-733,060 and substance P deletion inhibited TBI-induced oxidative stress and neuroinflammation. (A) Measurements of MDA levels. (B and C) The activities of GPx and SOD. (D and E) The expression levels of Interleukin-1ß (IL-1 ß) and TNF-α were measured by enzyme-linked immune-sorbent assay (ELISA). Data represent mean ± SEM (n = 6). $^{\#}P < 0.05$ vs. sham group and $^{*}P < 0.05$ vs. C57BL/6 J vehicle TBI group. C57, C57BL/6 J. SP-/-, SP−KO. NS, No significance.

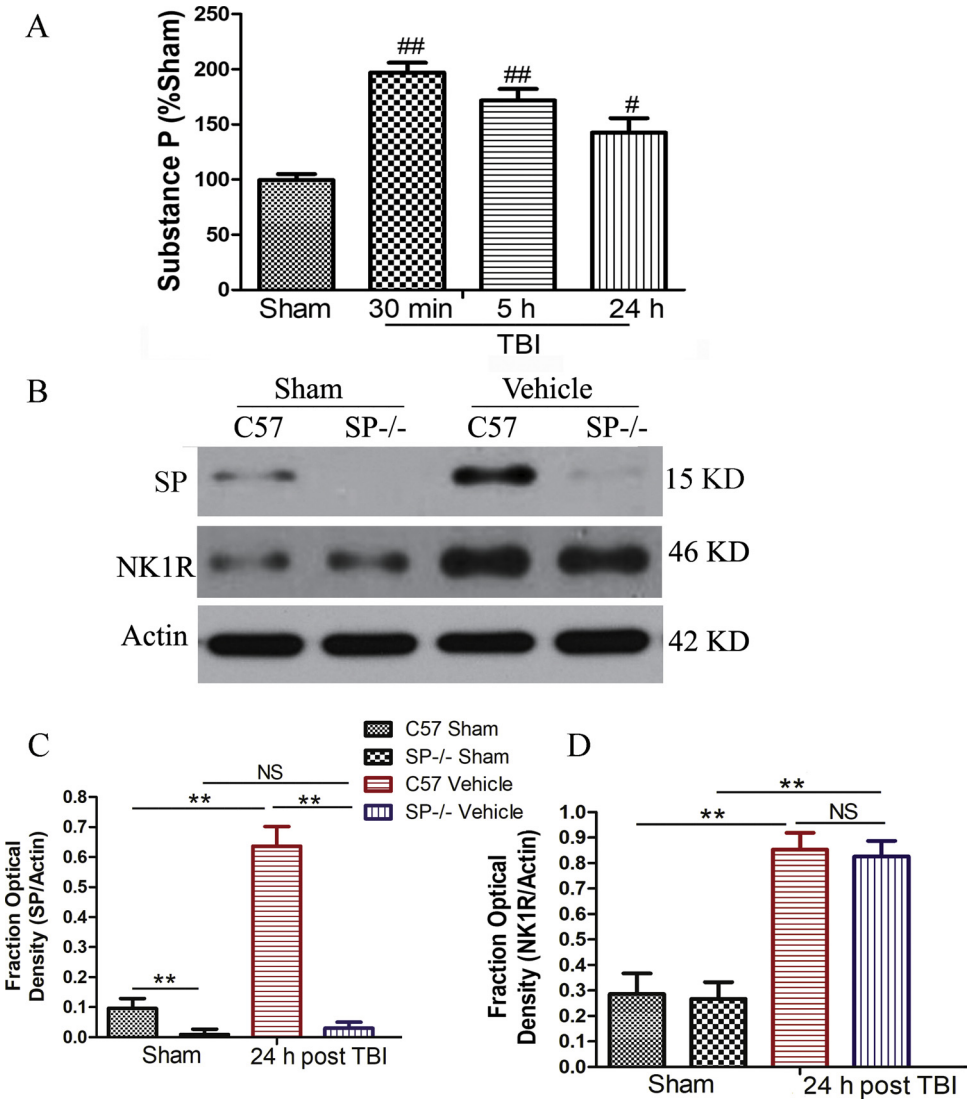

Fig. 5. The changes of serum SP concentration, and the levels of SP and NK1R expression in cortex after TBI. (A) The expression levels of serum SP in C57BL/6 J mice at 30 min, 5 h and 24 h after TBI were measured by substance P parameter assay kit (n = 6). $^{\#}P < 0.05$, $^{\#\#}P < 0.01$ vs. sham group. (B) The expression of SP and NK1R was detected with immunoblotting at 24 h post TBI. (C, D) Optical densities of the protein bands were analyzed with ChemiScope analysis and normalized with loading control (β-actin). Bars represent mean ± SEM (n = 4). $^{**}P < 0.01$. C57, C57BL/6 J. SP-/-, SP—KO. NS, No significance.

Whereas scratch injury-induced the upregulation of ROS production was inhibited both in L-733,060-treated C57BL/6 J group and in vehicle-treated SP-/- group (Fig. 6D).

3.7. L-733,060 and deletion of substance P diminished in vitro TBI-induced loss of mitochondrial membrane potential and ATP reduction

Given that the loss of ΔΨm, an important event involved in progression of mitochondrial dysfunction, leads to cell death of the host neuron (Chang and Johnson, 2012), we evaluated the depolarization of mitochondrial membrane potential (ΔΨm) of PCNs using rhodamine 123 and TMRM staining. The fluorescent signal, which displayed a punctuate pattern in healthy cells due to preferential staining of negatively charged mitochondria, became diffuse after scratch cell injury, presumably due to loss of ΔΨm (Fig. 7A and B). Whereas, L-733,060 treatment or deletion of SP decreased dissipation of ΔΨm induced by scratch cell injury (Fig. 7A and B).

In addition, the ATP content was determined quantitatively by evaluating its luminescence using an ATP-dependent bioluminescence assay kit. As presented in Fig. 7C, ATP content of cells in C57BL/6 J vehicle group was significantly decreased after scratch cell injury ($P < 0.01$). The ATP levels restored both in L-733,060-treated C57BL/6 J group and in vehicle-treated SP-/- group ($P < 0.05$, Fig. 7C).

4. Discussion

The results of the present study, in which the upregulation of serum SP levels was observe at 30 min. post-TBI and peaked at 5 h, then declined but remained elevated at 24 after TBI, are consistent with these earlier observations that serum levels of SP were elevated after TBI, with significant increases observed in both experimental (Donkin et al., 2009) and human TBI (Lorente et al., 2015). There is a significant increase in plasma SP concentration as early as 30 min post TBI and 5 h after injury in cerebral perivascular tissue with persisting for 24 h even 3 days following trauma (Cook et al., 2009; Donkin et al., 2009). By observing human postmortem TBI tissue and the rodent models, increased SP was apparent in cortical neurons and astrocytes (Donkin et al., 2009; Zacest et al., 2010). The increase in serum SP levels is associated with increased severity and mortality in patients (Lorente et al., 2015). Such increases in SP levels after TBI have been associated with increased permeability of the BBB and the formation of cerebral edema, together with the development of persistent motor and

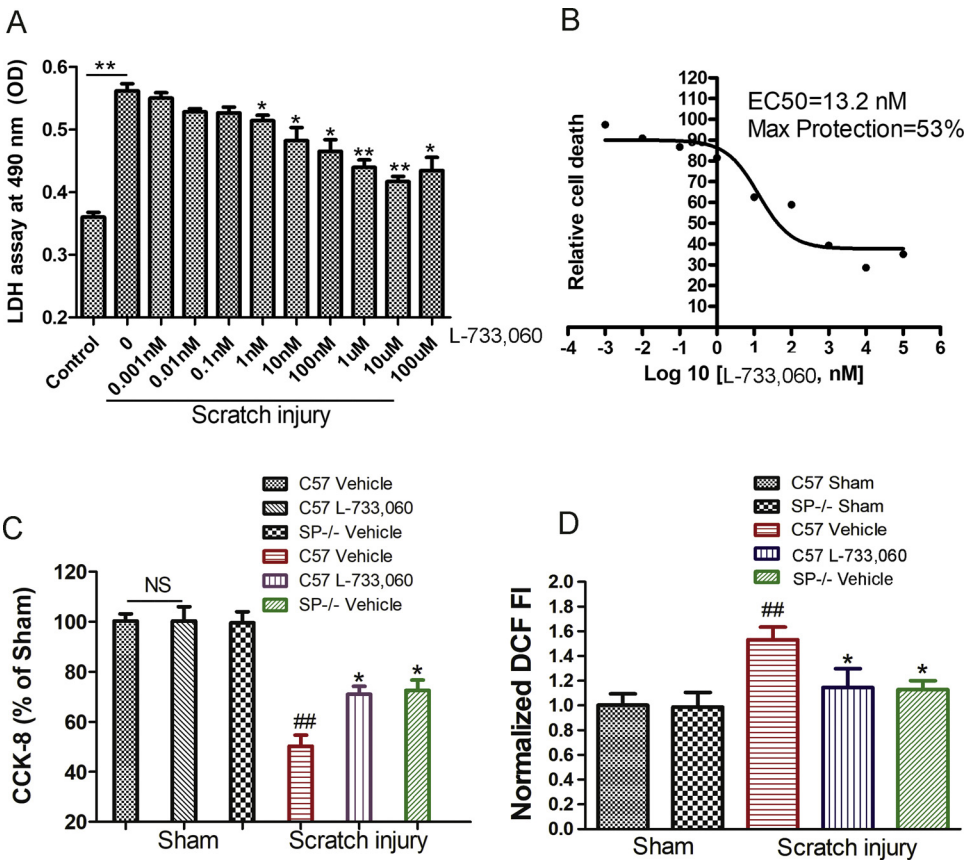

Fig. 6. L-733,060 and deletion of substance P inhibited *in vitro* TBI-induced cell death and ROS production. (A) PCNs were pre-incubated with L-733,060 for 2 h. Cell death was evaluated by LDH assay (n = 6). Data from three independent experiments are presented, and statistically significant differences are indicated with *P < 0.05 and **P < 0.01. (B) The resulting curves (plotted semi logarithmically) define the EC50 and maximum protection calculated by GraphPad Prism program. (C) Cell death was induced by scratch cell injury both in C57BL/6 J and SP-/- groups. L-733,060 was added to the culture medium 2 h prior to scratch cell injury in PCNs of C57BL/6 J group. Cell death was evaluated by CCK-8 assay (n = 6). ##P < 0.01 vs. C57BL/6 J vehicle sham group; *P < 0.05 vs. C57BL/6 J vehicle scratch injury group. (D) The levels of intracellular ROS generation were evaluated by DCFH-DA (n = 6). ##P < 0.01 vs. sham group; *P < 0.05 vs. C57BL/6 J vehicle scratch injury group. Results are expressed as the mean ± SEM with n = 6 per group. C57, C57BL/6 J. SP-/. SP—KO.

cognitive deficits (Donkin et al., 2009). Higher SP levels in serum and cortex were observed in wild type mice undergoing TBI relative to wild type sham group, but very little expression of cortical SP was detected in the SP-/- mice either TBI or not. The present study indicated TBI-induced the upregulation of SP levels only in wild type mice, and the loss of SP in SP-/- group maybe a consequence of SP deletion, independent of TBI.

Following release, SP can bind to tachykinin NK receptors to exert direct postsynaptic actions as a neurotransmitter or modulate other non-neuronal targets (Hokfelt et al., 2001). NK receptors are 7-transmembrane domain, G-protein-coupled receptors, with three, known as the NK1, NK2, and NK3 receptor, having been identified to date (Maggi, 1995). SP normally has the highest affinity for the NK1 receptor, and the predominance of the NK1 receptor is in the adult brain (Saffroy et al., 2003). The present study showed that a significant increase of NK1R protein levels following TBI was observed both in the wild type and the SP knock out mice, but there was no significantly difference in the expression of NK1R at 24 h post-TBI between these two groups, indicating upregulation of NK1R is a consequence of TBI, independent of the levels of substance P.

Neurokinin-1 receptor blockade studies have reported using NK1 receptor antagonists. In experimental studies, the efficacy of the NK1 antagonists in TBI has been demonstrated in both male and female animals (Corrigan et al., 2012). In particularly, the NK1-receptor antagonist NAT at 30 min post-injury improved free magnesium status after TBI, reduced BBB disruption and edema development (Donkin et al., 2009), indicating NAT acts presumably by competitive antagonism with SP for the NK1 receptor. SP release and binding to the NK1 receptor may influence functional outcome after TBI (Donkin et al., 2009). Rotarod performance was utilized as the motor strength and coordination outcome measure. Both the wire grip test and the rotarod test have been described earlier as the most sensitive test for the detection of motor deficits after rodent TBI (Hamm, 2001; Luo et al., 2010, 2011), and the NK1 receptor antagonist could alleviate TBI-induced motor deficits (Donkin et al., 2009). By using the wire grip test and the rotarod test, the attenuation of motor deficits in the SP-/- mice and in L-733,060-treated wild type mice was shown in the present study, suggesting deletion of SP or treatment with L-733,060 exerted a neuroprotective effect by alleviating motor deficits following TBI. Typical TBI patient also deficits in attention, memory, and behavioral control (Santopietro et al., 2015). Previous study demonstrated that neurokinin-1 receptor antagonist NAT had a positive effect on TBI-induced cognitive outcomes in rats, as assessed by the widely used MWM test (Donkin et al., 2011). The results of our study showed that TBI-induced spatial memory tasks deficits were alleviated in L-733,060-treated wild type mice (on days 10–15) and vehicle-treated SP-/- mice (on days 10–14), indicating that both L-733,060 and the deletion of SP could alleviate TBI-induced spatial memory deficits.

Cerebral edema has been reported to be one of the major factors leading to the high mortality and long-term disability associated with patients with TBI (Cui and Zhu, 2015). SP is the neuropeptide that is integrally linked to the increased vascular permeability and edema formation after TBI. In line with this notion, the observation of the present study further demonstrated both the BBB opening and the early vasogenic edema formation were attenuated in the SP knock out mice, and supports a direct role for SP in these events. In addition, activation of pro-inflammatory cytokines is an important neuroinflammatory response after TBI. Among proinflammatory cytokines, TNF-α and IL-1ß appear to play a determinant role in disrupting blood–brain barrier, and accelerating the formation of cerebral edema (Luo et al., 2013; Wang et al., 2007). The increase of TNF-α and IL-1ß levels has been observed in the brain parenchyma within the early hours after TBI in both humans and rodents (Winter et al., 2002). Inhibition of posttraumatic neurogenic inflammation by prior depletion of sensory neuropeptides using chronic capsaicin pretreatment attenuated BBB permeability, and the formation of edema and behavioral deficits (Nimmo et al., 2004). In

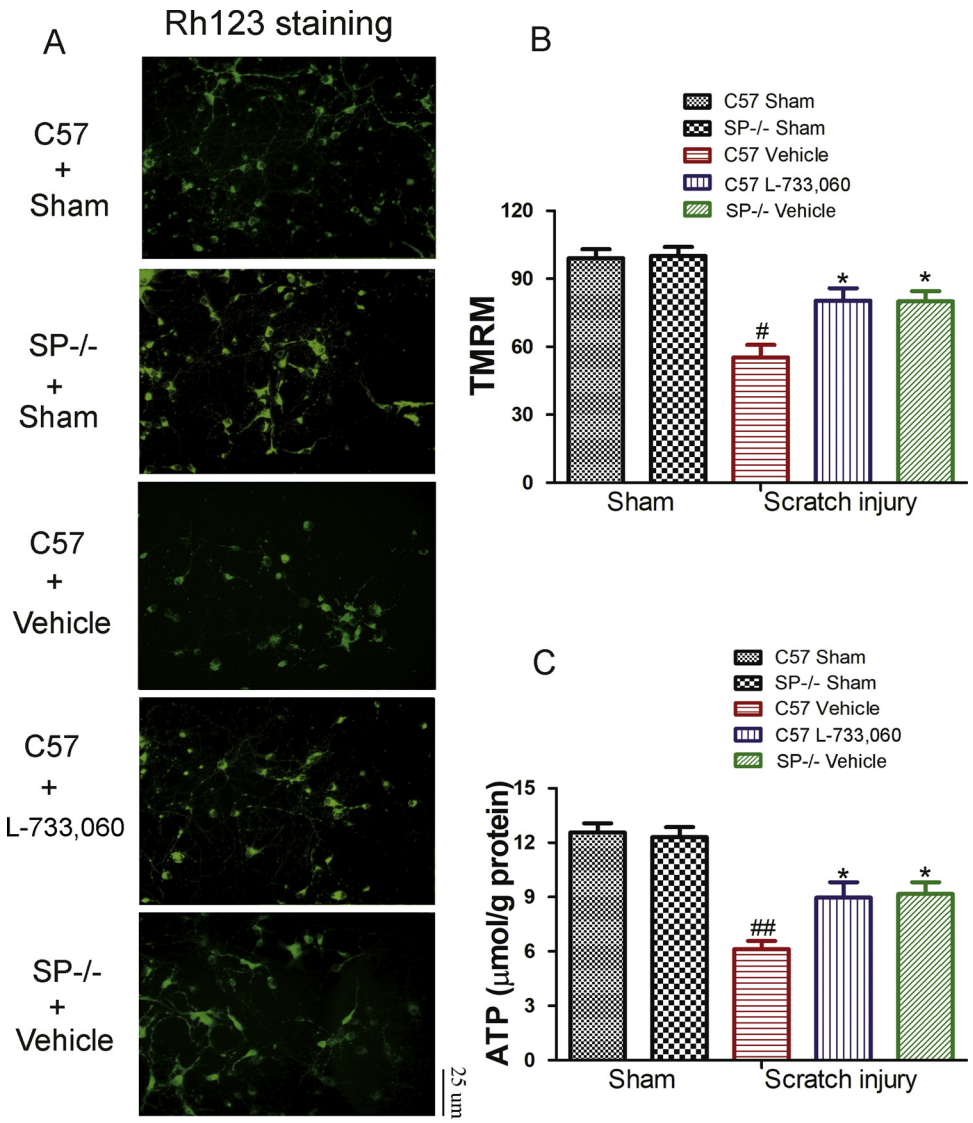

Fig. 7. L-733,060 and deletion of substance P diminished *in vitro* TBI-induced loss of mitochondrial membrane potential and ATP reduction. (A) The green fluorescence results from the accumulation of Rh 123 within negatively charged (functioning) mitochondria, displaying a punctuate pattern, as demonstrated in control cells. Compared with control cells, Rh 123 staining became diffuse, presumably due to the loss of ΔΨm mitochondrial depolarization after injury. The scale bar is 25 μm. (B) Semi-quantitative analysis of TMRM staining (n = 4). (C) The measurement of cellular ATP contents were determined by using a firefly luciferase ATP assay kit. $^{\#}P < 0.05$ and $^{\#\#}P < 0.01$ vs. sham group; $^{*}P < 0.05$ vs. C57BL/6 J vehicle scratch injury group. Results are expressed as the mean ± SEM with n = 4 per group. C57, C57BL/6 J. SP-/-, SP−KO. (For interpretation of the references to colour in this figure legend, the reader is referred to the web version of this article).

the present study, we found that following TBI, L-733,060 and knock out of SP significantly reduced the expression of two pro-inflammatory cytokines, IL-1β and TNF-α, thereby inhibiting the inflammatory response, indicating the anti-inflammatory effects of NK1R antagonist and SP knock out indeed existed in our TBI model. Moreover, SP could directly activate microglia and astrocytes by inducing the expression of NK1R on microglia and astrocytes (Corrigan et al., 2016). Following TBI, using NK1 antagonist, n-acetyl tryptophan (NAT) exerts neuroprotection via reducing the production of the proinflammatory cytokine IL-6 and inhibition of microglial proliferation (Carthew et al., 2012).

TBI caused profound tissue loss in the brain on day 7 and 17, and L-733,060 administration or SP deletion reduced the lesion volume at 17 days after TBI in the present study. TBI secondary injury is delayed and is thought to result from a combination of pathological factors after trauma. Evidences implies that apoptosis is an important type of cell death which may cause pathological changes and severe outcome post TBI (Wang et al., 2012). Specifically, mitochondria take part in intrinsic apoptotic pathway which involves a diverse of non-receptor-mediated stimuli producing intracellular signals (Elmore, 2007). Cytochrome c is a member of electron transport chain which participates in respiration, and the release of cytochrome c from mitochondria is a vital signal in apoptosis initiation (Babbitt et al., 2015). It is also known that cytochrome c is normally sequestered within mitochondrial cristae folds and mitochondrial cristae rearrangement allow the release of cytochrome (Estaquier and Arnoult, 2007). This release in turn activates downstream caspase such as caspase-3 to initiate apoptosis. Our data showed that L-733,060 and deletion of SP prevented cytochrome c release to cytoplasm and down-regulated the levels of cleaved caspase-3 at 24 h post-TBI, sequentially, restrained apoptosis occurring at a relatively early stage after TBI, indicating L-733,060 treatment or the deletion of substance P inhibited TBI-induced mitochondria mediated apoptosis pathway. *in vitro*, characterizing alterations in mitochondrial membrane potential (ΔΨm) is of great diagnostic value in predicting cell fate after TBI because mitochondria are known to play a major role in the regulation of cell death and survival (Nicholls and Budd, 2000). Rhodamin123 and TMRM are the reliable fluorescent probes for assessing changes of ΔΨm. Using rhodamine 123 staining and TMRM staining *in vitro*, we found that both L-733,060 and deletion of SP could moderate the dissipation of ΔΨm in mitochondria, thus indicating the protective effect of NK1R antagonist and SP knock out on scratch injury-induced mitochondrial membrane damage.

Substance P also primes polymorphonuclear cells for oxidative metabolism (superoxide production) (Hafstrom et al, 1998), thus providing a source of reactive oxygen species known to exacerbate the injury process. Oxidative stress plays a very important role in secondary injury induced by TBI, not only because of the excessive production of reactive oxygen species (ROS) but also due to the exhaustion of the endogenous antioxidant system. Several oxidants and their derivatives

are generated after TBI, which enhances the production of ROS along with the exhaustion of antioxidant defense enzymes, such as SOD, GPx and catalase (Özay et al., 2017). Both SOD and GPx are antioxidant enzymes that catalyze the reduction of glutathione (Halima et al., 2017). Lipid peroxidation, which refers to the oxidative degradation of lipids, increases membrane permeability, leading to cell damage. MDA has been utilized as an index of lipid peroxidation. The conversion of MDA and the activities of SOD and GPx in the cortex of mice with TBI in our study indicate that oxidative stress occurs following TBI. We also observed that the increase of the MDA level after TBI was mitigated, but the decrease in the activities of GPx and SOD was inhibited both in L-733,060-treated C57BL/6 J group and vehicle-treated SP−KO group, indicating that NK1R antagonist and deletion of substance P inhibited TBI-induced oxidative stress. In addition, a significant increase of MDA levels and a significant decrease of SOD activities after TBI were observed in vehicle-treated SP-/- group, relative to their respective sham SP-/- group, demonstrating TBI has a significant effect in the SP-/- mice when compared to SP-/- sham group. Moreover, L-733,060 and SP deletion by virtue of their antioxidant potential reduces oxidative stress (ROS production) generated due to scratch injury and helps the cells to maintain the cellular ATP levels, thus ultimately prevents cell death due to TBI *in vitro*.

In conclusion, our findings indicated that L-733,060 treatment or deletion of SP alleviated TBI-induced BBB disruption, brain edema and lesion volume, improved neurological function scores, as well as inhibited mitochondria mediated apoptotic pathway, oxidative insult and neuroinflammation. Upregulation of NK1R maybe a consequence of TBI, independent of the levels of substance P. This study raises the possibility that targeting SP or its receptor NK1R may have therapeutic efficacy in TBI, and more study is warranted for its clinical testing in the future.

Funding

This work was supported by the National Natural Science Foundation of China (No. 81400999, No. 81373251, No. 81530062), China Postdoctoral Science Foundation (No. 2014M551660), and a Project Funded by the Priority Academic Program Development of Jiangsu Higher Education Institutions (PAPD).

References

Babbitt, S.E., Sutherland, M.C., San Francisco, B., Mendez, D.L., Kranz, R.G., 2015. Mitochondrial cytochrome c biogenesis: no longer an enigma. Trends Biochem. Sci. 40 (Aug. (8)), 446–455.

Belayev, L., Busto, R., Zhao, W., Ginsberg, M.D., 1996. Quantitative evaluation of blood-brain barrier permeability following middle cerebral artery occlusion in rats. Brain Res. 739, 88–96.

Bermpohl, D., You, Z., Korsmeyer, S.J., Moskowitz, M.A., Whalen, M.J., 2006. Traumatic brain injury in mice deficient in Bid: effects on histopathology and functional outcome. J. Cereb. Blood Flow Metab. 26, 625–633.

Carthew, H.L., Ziebell, J.M., Vink, R., 2012. Substance P-induced changes in cell genesis following diffuse traumatic brain injury. Neuroscience 214, 78–83.

Chang, L.K., Johnson Jr., E.M., 2012. Cyclosporin A inhibits caspase-independent death of NGF-deprived sympathetic neurons: a potential role for mitochondrial permeability transition. J. Cell Biol. 157, 771–781.

Chodobski, A., Zink, B.J., Szmydynger-Chodobska, J., 2011. Blood-brain barrier pathophysiology in traumatic brain injury. Transl. Stroke Res. 2, 492–516.

Cook, N.L., Vink, R., Donkin, J.J., van den Heuvel, C., 2009. Validation of reference genes for normalization of real-time quantitative RT-PCR data in traumatic brain injury. J. Neurosci. Res. 87, 34–41.

Corrigan, F., Leonard, A., Ghabriel, M., Van Den Heuvel, C., Vink, R., 2012. A substance P antagonist improves outcome in female Sprague Dawley rats following diffuse traumatic brain injury. CNS Neurosci. Ther. 18, 513–515.

Corrigan, F., Mander, K.A., Leonard, A.V., Vink, R., 2016. Neurogenic inflammation after traumatic brain injury and its potentiation of classical inflammation. J. Neuroinflammation 13, 264.

Cui, T., Zhu, G., 2015. Ulinastatin attenuates brain edema after traumatic brain injury in rats. Cell Biochem. Biophys. 71, 595–600.

Dang, D.K., Shin, E.J., Kim, D.J., Tran, H.Q., Jeong, J.H., Jang, C.G., Nah, S.Y., Jeong, J.H., Byun, J.K., Ko, S.K., Bing, G., Hong, J.S., Kim, H.C., 2018. Ginsenoside Re protects methamphetamine-induced dopaminergic neurotoxicity in mice via upregulation of dynorphin-mediated κ-opioid receptor and downregulation of substance P-mediated neurokinin 1 receptor. J. Neuroinflammation 15, 52.

Donkin, J.J., Nimmo, A.J., Cernak, I., Blumbergs, P.C., Vink, R., 2009. Substance P is associated with the development of brain edema and functional deficits after traumatic brain injury. J. Cereb. Blood Flow Metab. 29, 1388–1398.

Donkin, J.J., Cernak, I., Blumbergs, P.C., Vink, R., 2011. A substance P antagonist reduces axonal injury and improves neurologic outcome when administered up to 12 hours after traumatic brain injury. J. Neurotrauma 28, 217–224.

Elmore, S., 2007. Apoptosis: a review of programmed cell death. Toxicol. Pathol. 35 (Jun. (4)), 495–516.

Estaquier, J., Arnoult, D., 2007. Inhibiting Drp1-mediated mitochondrial fission selectively prevents the release of cytochrome c during apoptosis. Cell Death Differ. 14 (Jun. (6)), 1086–1094.

Halima, B.H., Sonia, G., Sarra, K., Houda, B.J., Fethi, B.S., Abdallah, A., 2017. Apple cider vinegar attenuates oxidative stress and reduces the risk of obesity in high-fat-fed male Wistar rats. J. Med. Food 21 (1), 70–80.

Hamm, R.J., 2001. Neurobehavioral assessment of outcome following traumatic brain injury in rats: an evaluation of selected measures. J. Neurotrauma 18, 1207–1216.

Han, Z., Chen, F., Ge, X., Tan, J., Lei, P., Zhang, J., 2014. miR-21 alleviated apoptosis of cortical neurons through promoting PTEN-Akt signaling pathway in vitro after experimental traumatic brain injury. Brain Res. 1582, 12–20.

Hokfelt, T., Pernow, B., Wahren, J., 2001. Substance P: a pioneer amongst neuropeptides. J. Intern. Med. 249, 27–40.

Ji, J., Tyurina, Y.Y., Tang, M., Feng, W., Stolz, D.B., Clark, R.S., Meaney, D.F., Kochanek, P.M., Kagan, V.E., Bayır, H., 2012. Mitochondrial injury after mechanical stretch of cortical neurons in vitro: biomarkers of apoptosis and selective peroxidation of anionic phospholipids. J. Neurotrauma 29, 776–788.

Jin, Y., Lin, Y., Feng, J.F., Jia, F., Gao, G., Jiang, J.Y., 2015. Attenuation of cell death in injured cortex after post-traumatic brain injury moderate hypothermia: possible involvement of autophagy pathway. World Neurosurg. 84, 420–430.

Leonard, A.V., Vink, R., 2013. The effect of an NK1 receptor antagonist on blood spinal cord barrier permeability following balloon compression-induced spinal cord injury. Acta Neurochir. Suppl. 118, 303–306.

Liang, J., Wu, S., Xie, W., He, H., 2018. Ketamine ameliorates oxidative stress-induced apoptosis in experimental traumatic brain injury via the Nrf2 pathway. Drug Des. Devel. Ther. 12, 845–853.

Liao, Y., Liu, P., Guo, F., Zhang, Z.Y., Zhang, Z., 2013. Oxidative burst of circulating neutrophils following traumatic brain injury in human. PLoS One 8, e68963.

Lorente, L., Martín, M.M., Almeida, T., Hernández, M., Ramos, L., Argueso, M., Cáceres, J.J., Solé-Violán, J., Jiménez, A., 2015. Serum substance P levels are associated with severity and mortality in patients with severe traumatic brain injury. Crit. Care 19, 192.

Luo, C.L., Chen, X.P., Yang, R., Sun, Y.X., Li, Q.Q., Bao, H.J., Cao, Q.Q., Ni, H., Qin, Z.H., Tao, L.Y., 2010. Cathepsin B contributes to traumatic brain injury-induced cell death through a mitochondria-mediated apoptotic pathway. J. Neurosci. Res. 88, 2847–2858.

Luo, C.L., Li, B.X., Li, Q.Q., Chen, X.P., Sun, Y.X., Bao, H.J., Dai, D.K., Shen, Y.W., Xu, H.F., Ni, H., Wan, L., Qin, Z.H., Tao, L.Y., Zhao, Z.Q., 2011. Autophagy is involved in traumatic brain injury-induced cell death and contributes to functional outcome deficits in mice. Neuroscience 184, 54–63.

Luo, C.L., Chen, X.P., Li, L.L., Li, Q.Q., Li, B.X., Xue, A.M., Xu, H.F., Dai, D.K., Shen, Y.W., Tao, L.Y., Zhao, Z.Q., 2013. Poloxamer 188 attenuates in vitro traumatic brain injury-induced mitochondrial and lysosomal membrane permeabilization damage in cultured primary neurons. J. Neurotrauma 30, 597–607.

Luo, C., Li, Q., Gao, Y., Shen, X., Ma, L., Wu, Q., Wang, Z., Zhang, M., Zhao, Z., Chen, X., Tao, L., 2015. Poloxamer 188 Attenuates Cerebral Hypoxia/Ischemia Injury in Parallel with Preventing Mitochondrial Membrane Permeabilization and Autophagic Activation. J. Mol. Neurosci. 56, 988–998.

Maggi, C.A., 1995. The mammalian tachykinin receptors. Gen. Pharmacol. 26, 911–944.

Mannix, R.C., Zhang, J., Park, J., Zhang, X., Bilal, K., Walker, K., Tanzi, R.E., Tesco, G., Whalen, M.J., 2011. Age-dependent effect of apolipoprotein E4 on functional outcome after controlled cortical impact in mice. J. Cereb. Blood Flow Metab. 31, 351–361.

Mori, T., Wang, X., Jung, J.C., Sumii, T., Singhal, A.B., Fini, M.E., Dixon, C.E., Alessandrini, A., Lo, E.H., 2002. Mitogen-activated protein kinase inhibition in traumatic brain injury: in vitro and in vivo effects. J. Cereb. Blood Flow Metab. 22, 444–452.

Mustafa, A.G., Singh, I.N., Wang, J., Carrico, K.M., Hall, E.D., 2010. Mitochondrial protection after traumatic brain injury by scavenging lipid peroxyl radicals. J. Neurochem. 114, 271–280.

Nicholls, D.G., Budd, S.L., 2000. Mitochondria and neuronal survival. Physiol. Rev. 80 (Jan. (1)), 315–360.

Nimmo, A.J., Cernak, I., Heath, D.L., Hu, X., Bennett, C.J., Vink, R., 2004. Neurogenic inflammation is associated with development of edema and functional deficits following traumatic brain injury in rats. Neuropeptides 38, 40–47.

Özay, R., Türkoğlu, E., Gürer, B., Dolgun, H., Evirgen, O., Ergüder, B.İ., Hayırlı, N., Gürses, L., Şekerci, Z., Yılmaz, E.R., 2017. Does decorin protect neuronal tissue via its antioxidant and antiinflammatory activity from traumatic brain injury? An experimental study. World Neurosurg. 97, 407–415.

Park, S.Y., Marasini, S., Kim, G.H., Ku, T., Choi, C., Park, M.Y., Kim, E.H., Lee, Y.D., Suh-Kim, H., Kim, S.S., 2014. A method for generating a mouse model of stroke: evaluation of parameters for blood flow, behavior, and survival. Exp. Neurobiol. 23, 104–114.

Santopietro, J., Yeomans, J.A., Niemeier, J.P., White, J.K., Coughlin, C.M., 2015. Traumatic brain injury and behavioral health: the state of treatment and policy. N. C. Med. J. 76 (Apr. (2)), 96–100.

Saffroy, M., Torrens, Y., Glowinski, J., Beaujouan, J.C., 2003. Autoradiographic distribu-

tion of tachykinin NK2 binding sites in the rat brain: comparison with NK1 and NK3 binding sites. Neuroscience 116, 761–773.
Thornton, E., Vink, R., 2012. Treatment with a substance P receptor antagonist is neuroprotective in the intrastriatal 6-hydroxydopamine model of early Parkinson's disease. PLoS One 7, e34138.
Vink, R., van den Heuvel, C., 2010. Substance P antagonists as a therapeutic approach to improving outcome following traumatic brain injury. Neurotherapeutics 7, 74–80.
Vink, R., Young, A., Bennett, C.J., Hu, X., Connor, C.O., Cernak, I., Nimmo, A.J., 2003. Neuropeptide release influences brain edema formation after diffuse traumatic brain injury. Acta Neurochir. Suppl. 86, 257–260.
Wang, Q., Tang, X.N., Yenari, M.A., 2007. The inflammatory response in stroke. J. Neuroimmunol. 184, 53–56.
Wang, Y.Q., Wang, L., Zhang, M.Y., Wang, T., Bao, H.J., Liu, W.L., Dai, D.K., Zhang, L., Chang, P., Dong, W.W., Chen, X.P., Tao, L.Y., 2012. Necrostatin-1 suppresses autophagy and apoptosis in mice traumatic brain injury model. Neurochem. Res. 37 (Sep. (9)), 1849–1858.
Winter, C.D., Iannotti, F., Pringle, A.K., Trikkas, C., Clough, G.F., Church, M.K., 2002. Amicrodialysismethodfortherecoveryof IL-1beta, IL-6 and nerve growth factor from human brain in vivo. J. Neurosci. Methods 119, 45–50.
Wu, Q., Xia, S.X., Li, Q.Q., Gao, Y., Shen, X., Ma, L., et al., 2016. Mitochondrial division inhibitor1 (Mdivi-1) offers neuroprotection through diminishing cell death and improving functional outcome in a mouse model of traumatic brain injury. Brain Res. 1630, 134–143.
Wu, Q., Gao, C., Wang, H., Zhang, X., Li, Q., Gu, Z., Shi, X., Cui, Y., Wang, T., Chen, X., Wang, X., Luo, C., Tao, L., 2018. Mdivi-1 alleviates blood-brain barrier disruption and cell death in experimental traumatic brain injury by mitigating autophagy dysfunction and mitophagy activation. Int. J. Biochem. Cell Biol. 94, 44–55.
Yu, Z., Cheng, G., Huang, X., Li, K., Cao, X., 1997. Neurokinin-1 receptor antagonist SR140333: a novel type of drug to treat cerebral ischemia. Neuroreport 8, 2117–2119.
Yuan, F., Xu, Z.M., Lu, L.Y., Nie, H., Ding, J., Ying, W.H., Tian, H.L., 2016. SIRT2 inhibition exacerbates neuroinflammation and blood-brain barrier disruption in experimental traumatic brain injury by enhancing NF-κB p65 acetylation and activation. J. Neurochem. 136, 581–593.
Zacest, A.C., Vink, R., Manavis, J., Sarvestani, G.T., Blumbergs, P.C., 2010. Substance P immunoreactivity increases following human traumatic brain injury. Acta Neurochir. Suppl. 106, 211–216.